Time-Series InSAR Monitoring of Ground Deformation along the Baribis Fault Using LiCSBAS

Fadhila M.R [1*], Lestari D.[2]

[1] Undergraduate Student, Geodetic Engineering, Universitas Gadjah Mada, Indonesia

[2] Associate Professor, Geodetic Engineering, Universitas Gadjah Mada, Indonesia

* muhammad.rakha1803@mail.ugm.ac.id

Abstract: *The Baribis Fault, a significant seismic threat running through Java's densely populated northern regions, has yet to be mapped with a comprehensive 2D deformation analysis combining both ascending and descending Interferometric Synthetic Aperture Radar (InSAR) data. To better understand this risk, our study uses time-series InSAR to create a detailed map of its surface deformation. We analysed Sentinel-1 imagery from 2017 to 2023 using the Small Baseline Subset (SBAS) technique within the open-source LiCSBAS platform, with further analysis performed in Jupyter Notebook. By combining data from ascending and descending satellite paths, we decomposed the line-of-sight displacement into true vertical and horizontal (East-West) ground motion. The accuracy of our results was then confirmed by comparing them against measurements from two nearby CORS stations (CBTU and CTGR), yielding a Root Mean Square Error between 5.09 and 5.34 cm. Our analysis reveals complex ground motion: vertical displacement rates range from -86.4 to +32 mm·yr^{-1}, showing uplift in the north and nearly subsidence in the south, while horizontal velocities range from -8.6 to 10.6 mm·yr^{-1}, indicating a clear left-lateral strike-slip pattern. Beyond providing the first comprehensive 2D deformation map for this critical fault, this research highlights the practical power of a fully open-source workflow. It shows how community-driven tools and free satellite data make advanced geodetic monitoring more accessible, empowering local institutions to conduct their vital hazard assessments. This work ultimately demonstrates how collaborative open science in remote sensing can directly contribute to building more resilient communities.*

Keywords: *Baribis Fault, Deformation, InSAR, LiCSBAS, Open Science, SBAS*

Introduction

The northwestern region of Java, Indonesia, stands as a critical intersection of high tectonic activity and dense urbanization, hosting major metropolitan areas such as Jakarta and Bekasi. Indonesia's complex geological setting, located at the confluence of four major tectonic plates—the Eurasian, Indo-Australian, Philippine Sea, and Pacific plates—results in a high degree of seismicity throughout the archipelago (Koulali et al., 2016; PuSGeN, 2017). This activity exposes the region to significant seismic hazards originating from shallow crustal faults. Among these, the Baribis Fault is a primary source of concern, officially recognized as a major active fault structure within the national seismic hazard map and stretching approximately 100 km across vital economic and population centers (Widiyantoro et al., 2022; Marliyani et al., 2016). The urgency of monitoring this fault was recently underscored by the M 4.7 earthquake in August 2025, which was strongly felt

across the region and sparked scientific discussion regarding its source within the larger Java Back-arc Thrust system, of which the Baribis Fault is a major component (Ramdhani, 2025; Wafid, 2025). This event serves as a stark reminder of the fault's active status and the accumulating tectonic strain (Widiyantoro et al., 2022).

Historically, the Baribis Fault has been linked to destructive earthquakes in 1780 and 1834 (Nguyen et al., 2015). However, a notable lack of significant recorded seismicity in recent decades has led to the hypothesis of a "seismic gap," suggesting that a segment of the fault is likely in a locked state where strain energy is continuously accumulating. Previous research has consistently pointed towards this potential. Studies using borehole seismometers and GPS data have revealed differing seismicity characteristics between the fault's western segment near Jakarta and its eastern segment, indicating a complex and not yet fully understood deformation mechanism (Gunawan & Widiyantoro, 2019; Widiyantoro et al., 2022; Damanik et al., 2021). Geodetic studies using GNSS have successfully indicated ongoing crustal movement and strain accumulation in the region, with horizontal movement rates estimated between 0.96 to 6.85 mm/year (Gunawan & Widiyantoro, 2019; Koulali et al., 2017; Susilo et al., 2022). Furthermore, analysis of GPS data has identified significant compression, up to -3 microstrain/year, concentrated in the western segment, reinforcing the interpretation of a locked zone accumulating elastic energy (Widiyantoro et al., 2022).

Despite these crucial insights, existing studies face a primary limitation: the sparse spatial coverage of ground-based methods like GNSS. While highly accurate at specific points, the wide spacing between stations makes it difficult to capture the complete spatial variability of deformation along the fault. This data gap hinders a comprehensive identification of strain accumulation patterns, leaving a critical blind spot in seismic hazard assessment. Gunawan & Widiyantoro (2019) specifically highlighted the need for more detailed studies to determine key fault parameters like *slip rate* and *locking depth*, which have not been extensively explored using high-resolution spatial data. While some InSAR studies have been conducted, they have often been limited to one-dimensional or localized analysis without a full 2D decomposition across the primary segments of the fault (Khakim et al., 2023; Suhadha et al., 2023; Fuadi et al., 2020) Enhancing such analyses requires robust satellite systems, as demonstrated by applications of the SMART method in vendor selection for Indonesia’s Remote Sensing Satellite Systems (InaRSSat), which supports efficient procurement and deployment of SAR technologies for national hazard monitoring (Sadly et al., 2018).

To address this research gap, this study utilizes InSAR with the SBAS technique to create the first comprehensive 2D surface deformation map of the Baribis Fault's most critical segments. By integrating Sentinel-1 data from both ascending and descending satellite orbits between 2017 and 2024, we decompose the fundamental one-dimensional line-of-sight (LOS) measurements into true vertical (Up-Down) and horizontal (East-West) ground motion, providing a more robust characterization of the fault's movement (Bürgmann et al., 2000). To ensure the reliability of our results, the vertical displacement component is validated against continuous GNSS measurements from the CBTU and CTGR CORS stations (Susilo et al., 2023). The primary objective of this research is to quantify the 2D displacement and velocity fields along the Jakarta and Bekasi-Purwakarta segments, providing critical data for enhancing seismic hazard models and supporting risk-aware infrastructure planning in one of Indonesia's most vital regions.

Methodology

2.1. Study Area and Datasets

The study area focuses on the Jakarta and Bekasi-Purwakarta segments of the Baribis Fault. The area of interest is geographically bounded by coordinates from 106°24' E to 107°33' E and 6°17' S to 6°32' S.

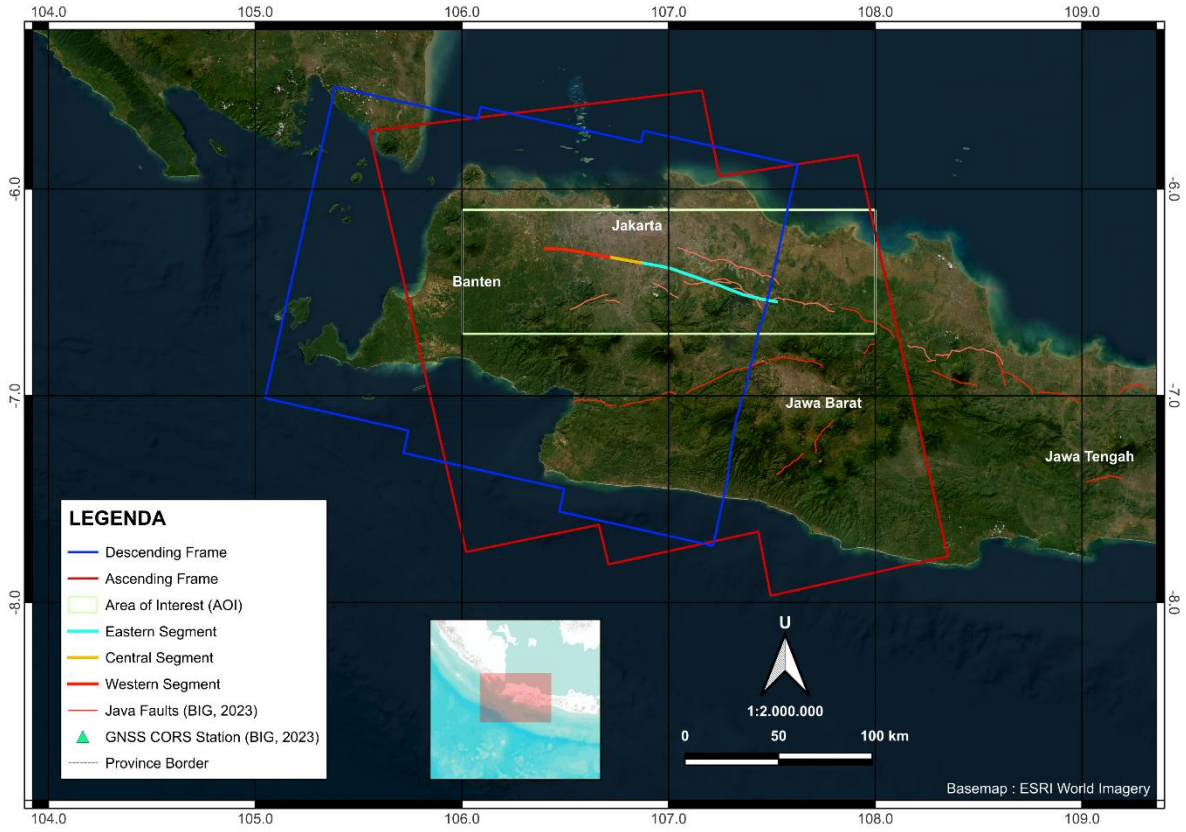

Figure 1: Study area in this research.

The primary data for this research consists of C-band Sentinel-1 Synthetic Aperture Radar (SAR) imagery, which not only enables tectonic deformation monitoring but also supports advanced applications like scattering models for oil palm phenology using multi-band polarimetric data, highlighting its utility in diverse environmental contexts (Darmawan et al., 2021). This imagery was obtained as pre-processed L2 unwrapped interferograms and coherence maps from the COMET LiCSAR portal. To enable a comprehensive 2D analysis, data from two separate orbital tracks were utilized. For the ascending orbit (Frame 098A_09673_121312), a total of 669 interferograms covering the period from January 17, 2017, to October 31, 2024, were processed. Complementing this, 690 interferograms from the descending orbit (Frame 047D_09652_111009) were used, covering the period from January 1, 2017, to June 30, 2023.

Several ancillary datasets were crucial for processing and validation. Tropospheric correction data from the Generic Atmospheric Correction Online Service for InSAR (GACOS) were applied to mitigate atmospheric phase delays. For independent validation, 3D displacement time-series from two Continuously Operating Reference Stations (CORS), namely Cibitung (CBTU) and Tangerang (CTGR), were used. This GNSS data, processed within the ITRF2014 reference frame, covers the period from 2017 to 2021 and was obtained from the study by Susilo et al. (2023).

2.2 InSAR Time-series Processing

The ground deformation time-series was derived using the Small Baseline Subset (SBAS) technique, a powerful InSAR method for monitoring slow-moving surface displacement over large areas (Berardino et al., 2002). The entire processing workflow was implemented using the open-source LiCSBAS (Morishita et al., 2020). The fundamental principle of InSAR is that the phase difference (ϕ_{int}) in an interferogram is a sum of several components, including topography (ϕ_{topo}), atmospheric delay (ϕ_{atm}), orbital errors (ϕ_{orb}), noise (ϕ_{noise}), and the signal of interest - surface deformation (ϕ_{def}). The relationship can be expressed as (Bouraoui, 2013):

$$\phi_{int} = \phi_{topo} + \phi_{def} + \phi_{atm} + \phi_{orb} + \phi_{noise} + \phi_{scat} \quad (1)$$

The primary goal of the time-series processing is to isolate the deformation component (ϕ_{def}) from the other signals. The workflow began with the direct use of the pre-processed unwrapped interferograms from LiCSAR, maintaining their full spatial resolution of

approximately 100 meters. A crucial initial step was the application of GACOS data to correct for tropospheric phase delays, a significant source of error in tropical climates (Yu et al., 2018).

Before the main inversion, a critical quality control step was performed using loop closure to ensure network consistency. This method identifies interferograms with significant phase unwrapping errors by summing the phase values within closed loops of three interferograms (e.g., A-B, B-C, C-A). For a consistent network, the closure phase (Φ_{loop}) should be near zero, as shown in equation (2) below (Biggs et al., 2007).

$$\Phi_{loop} = \phi_{AB} + \phi_{BC} - \phi_{AC} \approx 0 \quad (2)$$

Interferograms contributing to loops with a closure phase error exceeding a threshold of 2.5 radians were discarded. The resulting refined and consistent network of interferograms was then inverted using a NSBAS Least Squares (LS) algorithm (Doin et al., 2011). This process solves the system of linear equations $d = G.m$, where d is the vector of unwrapped phase values for each interferogram, m is the vector of incremental displacements to be solved, and G is the design matrix linking the two.

Finally, the raw time-series results were refined through post-processing. A mask was applied to exclude low-quality pixels based on statistical criteria such as low mean coherence (<0.1) and high velocity standard deviation. A spatio-temporal filter (5 km spatial radius) was then applied to the masked results to remove residual noise and long-wavelength orbital ramp errors, thereby isolating the tectonic deformation signal more clearly (Morishita et al., 2020).

2.3. Decomposition to 2D Velocity

A fundamental limitation of InSAR is that it measures displacement only in the one-dimensional LOS direction. To obtain a more comprehensive understanding of the ground motion, the LOS velocity maps from both the ascending and descending orbits were combined. This integration allows for the decomposition of the 1D measurements into two independent components: true vertical (Up-Down) and horizontal (East-West) ground motion. This is possible due to the different viewing geometries of the two satellite tracks, while acknowledging the near-zero sensitivity of the near-polar Sentinel-1 orbits to North-South motion.

2.4. Validation with GNSS CORS

To independently assess the accuracy of the InSAR-derived results, the vertical deformation component was validated against the ground-truth measurements from the CBTU and CTGR CORS stations. The vertical displacement time-series was extracted from the InSAR data at the pixel nearest to each station's location. This InSAR time-series was then compared with the daily vertical time-series from the GNSS data. Given the fundamental difference in reference frames—InSAR being relative to the first acquisition and a reference point, while GNSS is tied to an absolute global frame (ITRF2014)—the comparison focused on the consistency of temporal trends and variability. The Root Mean Square Error (RMSE) was calculated to quantify the overall difference between the two datasets, providing a measure of the accuracy of the InSAR results.

Results and Discussion

This section presents the surface deformation velocity fields derived from the InSAR time-series analysis of Sentinel-1 data from 2017 to 2024. The results are presented first as one-dimensional Line-of-Sight (LOS) velocities, which are then decomposed into two-dimensional (2D) vertical and horizontal components. This is followed by a detailed discussion interpreting the fault kinematics and comparing the findings with the established national seismic hazard framework.

3.1. LOS and 2D Velocity

The mean surface velocity in the satellite's LOS direction is presented in Figure 1. Negative values (blue) indicate motion away from the satellite, while positive values (brown) represent motion towards the satellite. Both the ascending (Fig. 1a) and descending (Fig. 1b) tracks show a consistent large-scale pattern: the block north of the Baribis Fault predominantly exhibits positive LOS velocity (movement towards the satellite), whereas the southern block shows a gradual negative trend. Superimposed on this regional pattern are distinct, localized zones of strong negative velocity (> -50 mm/year) concentrated over the urban centers of Jakarta and Bekasi.

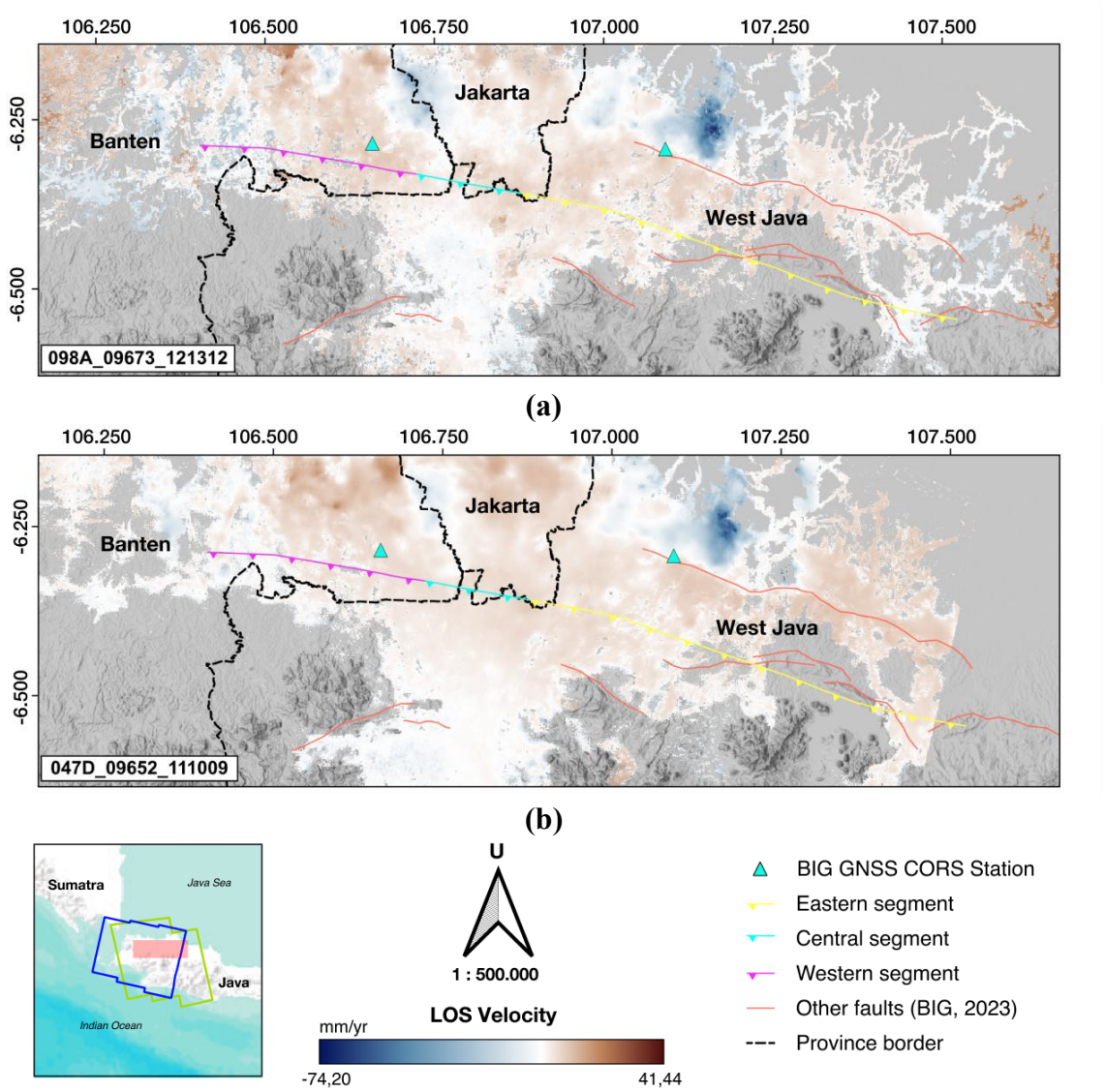

Figure 3: LOS velocity maps from (a) ascending and (b) descending Sentinel-1 tracks for the period 2017–2024.

To better isolate and interpret the ground motion, the LOS velocities were decomposed into vertical (Up-Down, UD) and horizontal (East-West, EW) components, as shown in Figure 2. The horizontal velocity field (Fig. 2a) reveals a distinct shear pattern across the Baribis Fault, with the northern block moving westward and the southern block moving eastward at rates ranging from -8.6 to +10.6 mm/year. The vertical velocity field (Fig. 2b) shows a clear regional trend of uplift in the northern block and subsidence in the southern block, with rates ranging from -86.4 to +32 mm/year. This tectonic signal is partially obscured by the intense, localized subsidence in Jakarta and Bekasi.

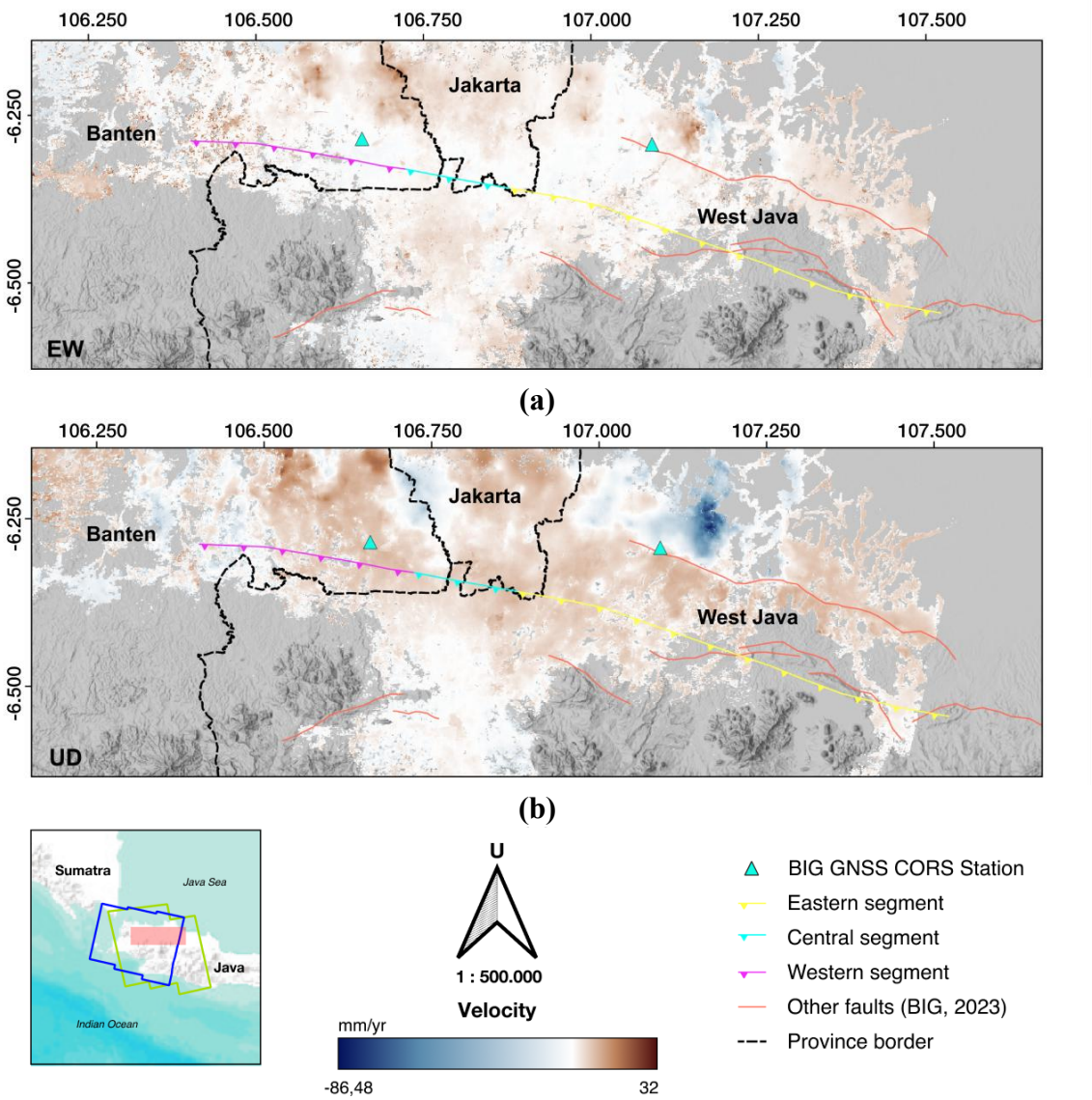

Figure 3: Decomposed 2D velocity maps showing (a) East-West and (b) Up-Down ground motion.

The observed EW velocity pattern is kinematically consistent with a left-lateral (sinistral) strike-slip mechanism along the Baribis Fault. This finding provides a spatially continuous confirmation of the fault's behavior, which aligns with previous seismological studies that identified a sinistral component (Damanik et al., 2021; Daryono et al., 2021). The quantification of this horizontal motion across a wide area is critical for understanding strain partitioning and assessing the seismic hazard posed by the fault, which is believed to be capable of generating large-magnitude earthquakes.

Analysis of the vertical motion reveals two superimposed signals. The most prominent signal is the severe subsidence in Jakarta and Bekasi, which is attributed to non-tectonic, anthropogenic processes such as excessive groundwater extraction and infrastructure loading on unconsolidated alluvial deposits. This observation is consistent with numerous

prior studies on land subsidence in the region (Abidin et al., 2011; Agustan et al., 2022). While this anthropogenic signal is significant, the underlying tectonic deformation pattern is also discernible. Outside the main subsidence bowls, the general uplift of the northern block relative to the southern block is characteristic of a thrust fault mechanism, where the hanging wall (north) moves up relative to the footwall (south). This interpretation is supported by general fault mechanics (Wright et al., 2004) and is consistent with focal mechanism solutions from local earthquakes that indicate thrusting near Jakarta (Widiyantoro et al., 2022). This observation is also consistent with the classification of the Baribis Fault in the Pusgen 2017, where it is defined as a major back-arc thrust system that forms part of a larger continuous structure including the Kendeng Fault Zone in Central and East Java. The national map officially delineates segments such as the Subang and Cirebon segments as reverse faults with a southerly dip of approximately 45°, a geometric characteristic that aligns with the uplift pattern observed in our data.

The synthesis of both the horizontal and vertical components provides a comprehensive view of the fault's kinematics. The coexistence of a significant left-lateral strike-slip motion with a clear thrust component strongly supports the interpretation that the Baribis Fault in this segment operates as an oblique thrust fault. This 2D deformation map provides the first spatially detailed geodetic evidence that confirms the complex faulting mechanism previously suggested by seismological studies (Damanik et al., 2021; Daryono et al., 2021).

The synthesis of both horizontal and vertical components provides a comprehensive view of the fault's kinematics. The coexistence of a significant left-lateral strike-slip motion with a clear thrust component strongly supports the interpretation that the Baribis Fault in this segment operates as an oblique thrust fault. This 2D deformation map provides the first spatially detailed geodetic evidence that confirms the complex faulting mechanism previously suggested by seismological studies (Damanik et al., 2021; Daryono et al., 2021).

Furthermore, the geodetic slip rates derived from GPS in the national hazard report, estimated between 2.3 to 5.6 mm/year for the broader Baribis-Kendeng system, provide a valuable reference for the deformation rates observed in this study, although our high-resolution InSAR data reveals more detailed spatial variations in velocity.

3.2. Validation using GNSS CORS Station

To independently assess the accuracy and reliability of the InSAR-derived vertical deformation, the time-series results were compared against high-precision, ground-truth measurements from two permanent GNSS CORS stations: Cibitung (CBTU) and

Tangerang (CTGR). It is important to note that InSAR provides relative displacement measurements (referenced to the first acquisition and a stable point), while GNSS provides absolute displacement within a global reference frame (ITRF2014) (Susilo et al., 2023). Therefore, this validation focuses on evaluating the consistency of the temporal trends and overall variability between the two datasets, rather than their absolute values.

The quantitative results of this comparison are summarized in Table 2. The Root Mean Square Error (RMSE) between the InSAR and GPS time-series at the CBTU station was calculated to be 3.89 cm for the ascending track and 3.80 cm for the descending track. The discrepancy was more pronounced at the CTGR station, which yielded a higher RMSE of 6.07 cm (ascending) and 6.51 cm (descending). The overall RMSE for the validation was approximately 5.1 cm to 5.3 cm.

Table 1: Statistical comparison of vertical displacement from InSAR and GPS, showing Standard Deviation (SD) and Root Mean Square Error (RMSE) in cm.

Station	**Displacement SD (cm)**			**RMSE$_{InSAR\ v\ CORS}$ (cm)**	
	Ascending	*Descending*	*CORS*	*Ascending*	*Descending*
CBTU	1,354	1,254	0,981	3,885	3,796
CTGR	1,404	0,870	1,371	6,065	6,507
Overall	**1,379**	**1,129**	**1,190**	**5,097**	**5,338**

The quantitative results of this comparison are summarized in Table 2. The Root Mean Square Error (RMSE) between the InSAR and GPS time-series at the CBTU station was calculated to be 3.89 cm for the ascending track and 3.80 cm for the descending track. The discrepancy was more pronounced at the CTGR station, which yielded a higher RMSE of 6.07 cm (ascending) and 6.51 cm (descending). The overall RMSE for the validation was approximately 5.1 cm to 5.3 cm.

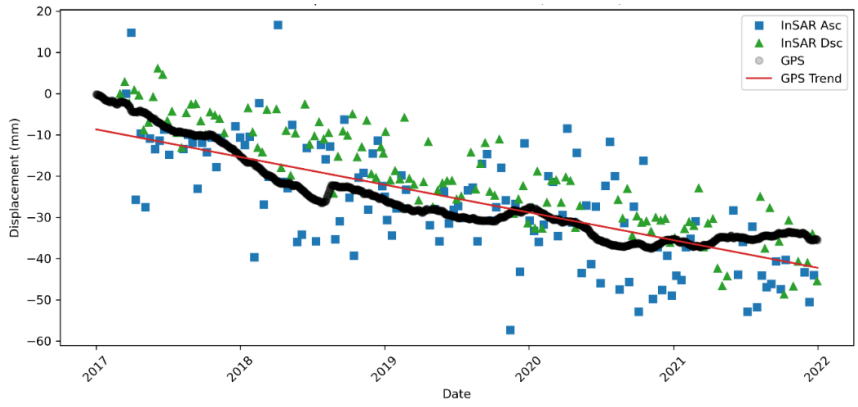

(a)

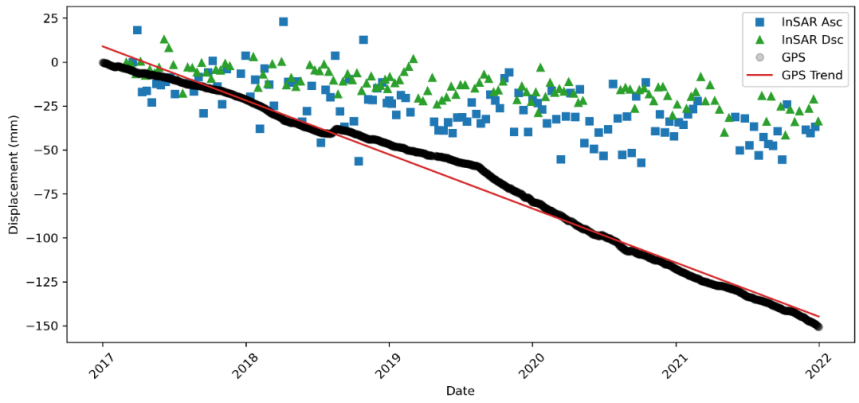

(b)

Figure 3: Comparison of vertical displacement time-series from InSAR (ascending and descending) and GPS at stations (a) CBTU and (b) CTGR from 2017 to 2021.

In contrast, the comparison at the CTGR station (Fig. 3b) reveals a more significant deviation. While the GPS data shows a clear and accelerating subsidence trend, the InSAR time-series exhibits a much flatter and noisier signal that fails to capture the full magnitude of the ground motion. This larger discrepancy, which is reflected in the higher RMSE values at this station, suggests that the InSAR signal quality at this specific location may be compromised, potentially by localized atmospheric effects or surface characteristics that reduce signal coherence.

In summary, the validation exercise indicates that the InSAR-SBAS method successfully identified the general regional deformation trend (i.e., subsidence) across the study area. However, the RMSE values of 3.8 cm to 6.5 cm highlight the existence of significant localized inaccuracies when comparing the satellite-based area measurements (a ~100 m pixel) with the precise point measurements of a GNSS antenna. These discrepancies are likely attributable to a combination of factors, including the inherent spatial averaging of InSAR, residual uncorrected atmospheric noise, and the different reference frames. Therefore, while the InSAR results provide an invaluable, spatially continuous view of the regional deformation patterns, this validation underscores the importance of interpreting the absolute magnitude of displacement at any specific point with caution.

3.3. Study Limitations

It is important to acknowledge several limitations inherent in this study's methodology and data that provide context for the results. Firstly, this research utilized pre-processed unwrapped interferograms from the COMET LiCSAR service. While this approach enables highly efficient, large-scale time-series analysis and provides a robust regional overview, it is dependent on the standardized processing parameters of the LiCSAR pipeline.

Consequently, this study did not involve interferogram pre-processing from raw SAR data, which would have allowed for customized strategies like targeted filtering or multi-looking to potentially enhance signal quality in specific areas with challenging surface conditions. This may contribute to some of the noise observed in the final velocity fields.

Secondly, a significant limitation relates to the dimensionality of the deformation measurements. Due to the near-polar orbit of the Sentinel-1 satellite, our InSAR analysis is largely insensitive to the North-South component of ground motion. Although the resulting 2D (East-West and Up-Down) velocity field successfully captures the primary kinematics of the left-lateral and thrust components of the Baribis Fault, a complete 3D deformation field would be necessary to fully resolve the fault's oblique motion.

Finally, despite the application of GACOS for atmospheric correction, residual tropospheric noise remains a significant challenge, particularly in Indonesia's humid tropical climate. This residual noise is a likely contributor to the data scatter in the InSAR time-series and the observed discrepancies in the validation against GNSS CORS data. The validation itself was methodologically limited to comparing temporal trends, as the fundamental difference in reference frames—relative for InSAR versus absolute for GNSS—prevents a direct comparison of absolute displacement values. These factors should be considered when interpreting the precise magnitude of deformation at any specific location.

Conclusion and Recommendation

This study successfully generated the first comprehensive 2D surface deformation map for the Jakarta and Bekasi-Purwakarta segments of the Baribis Fault using time-series InSAR analysis of Sentinel-1 data from 2017 to 2024. The results reveal a complex oblique thrust faulting mechanism, which was previously suggested by seismological studies but is now confirmed with spatially continuous geodetic data. The horizontal velocity field clearly indicates a left-lateral strike-slip motion, with rates ranging from -8.6 to +10.6 mm/year. This is coupled with a vertical component showing regional uplift of the northern block relative to the southern block, a characteristic of thrust faulting that is highly consistent with the fault's classification in Indonesia's national hazard map. The validation against GNSS CORS data confirmed that the InSAR results effectively capture the long-term regional deformation trends, although localized discrepancies, with an overall RMSE of 5.1 to 5.3 cm, were observed. Ultimately, this research provides an invaluable, spatially continuous dataset that clarifies the current kinematics of a critical active fault. These findings contribute crucial high-resolution data that can be used for future updates of national seismic

hazard models, such as those coordinated by the National Center for Earthquake Studies (PuSGeN), thereby supporting risk mitigation strategies in the densely populated Jakarta metropolitan area.

References

Abidin, H. Z., Andreas, H., Gumilar, I., Fukuda, Y., Pohan, Y. E., & Deguchi, T. (2011). Land Subsidence of Jakarta (Indonesia) and Its Relation with Urban Development. *Natural Hazards, 59*(3), 1753-1771. https://doi.org/10.1007/s11069-011-9866-9

Agustan, A., Ito, T., Kriswati, E., Priyadi, H., Sadmono, H., & Hernawati, R. (2022). Time Series InSAR Analysis Over Jakarta Metropolitan Area. In *2022 IEEE Asia-Pacific Conference on Geoscience, Electronics and Remote Sensing Technology (AGERS)* (pp. 30-35). IEEE.

Berardino, P., Fornaro, G., Lanari, R., & Sansosti, E. (2002). A New Algorithm for Surface Deformation Monitoring Based on Small Baseline Differential SAR Interferograms. *IEEE Transactions on Geoscience and Remote Sensing, 40*(11), 2375-2383. https://doi.org/10.1109/TGRS.2002.803792

Biggs, J., Wright, T., Lu, Z., & Parsons, B. (2007). Multi-interferogram method for measuring interseismic deformation: Denali Fault, Alaska. *Geophysical Journal International*, *170*(3), 1165–1179.

Bürgmann, R., Rosen, P. A., & Fielding, E. J. (2000). Synthetic Aperture Radar Interferometry to Measure Earth's Surface Topography and Its Deformation. *Annual Review of Earth and Planetary Sciences, 28*, 169-209. https://doi.org/10.1146/annurev.earth.28.1.169

Damanik, R., Supendi, P., Widiyantoro, S., Rawlinson, N., Ardianto, A., Gunawan, E., Husni, Y. M., Zulfakriza, Z., Sahara, D. P., & Shiddiqi, H. A. (2021). Earthquake Monitoring of the Baribis Fault Near Jakarta, Indonesia, Using Borehole Seismometers. *Geoscience Letters, 8*(1), 37. https://doi.org/10.1186/s40562-021-00209-4

Darmawan, S., Carolita, I., Hernawati, R., Dirgahayu, D., Agustan, A., Permadi, D. A., Sari, D. K., Suryadini, W., Wiratmoko, D., & Kunto, Y. (2021). The potential scattering model for oil palm phenology based on spaceborne X-, C-, and L-band polarimetric SAR imaging. Journal of Sensors, 2021, Article 6625774, 14 pages. https://doi.org/10.1155/2021/6625774

Daryono, M. R., Natawidjaja, D. H., Puji, A. R., & Aribowo, S. (2021). Fault Rupture in Baribis Fault Possibly Related to the 1847 Major Earthquake Event in the Cirebon Area. *IOP Conference Series: Earth and Environmental Science, 873*(1), 012052. https://doi.org/10.1088/1755-1315/873/1/012052

Doin, M.-P., Guillaso, S., Jolivet, R., Lasserre, C., Lodge, F., Ducret, G., & Grandin, R. (2011). Presentation of the small baseline NSBAS processing chain on a case example: The Etna deformation monitoring from 2003 to 2010 using Envisat data. In *Proceedings of the fringe symposium* (pp. 3434–3437).

Fuadi, F. Z., Kuncoro, H., Wibowo, S. T., & Rizqiansyah, A. (2020). Slip Deficit Rates Estimation at Baribis Fault on 2016-2019 GPS Observations. *Prosiding FTSP Series*.

Gunawan, E., & Widiyantoro, S. (2019). Active Tectonic Deformation in Java, Indonesia Inferred from a GPS-Derived Strain Rate. *Journal of Geodynamics, 123*, 49–54. https://doi.org/10.1016/J.JOG.2019.01.004

Khakim, M. Y. N., Supardi, S., & Tsuji, T. (2023). Earthquake Affects Subsidence in Jakarta Using Sentinel-1A Time Series Images and 2D-MSBAS Method. *Vietnam Journal of Earth Sciences, 45*(1), 111–128. https://doi.org/10.15625/2615-9783/18021

Koulali, A., McClusky, S., Susilo, S., Leonard, Y., Cummins, P., Tregoning, P., Meilano, I., Efendi, J., & Wijanarto, A. B. (2017). The Kinematics of Crustal Deformation in Java from GPS Observations: Implications for Fault Slip Partitioning. *Earth and Planetary Science Letters, 458*, 69–79. https://doi.org/10.1016/J.EPSL.2016.10.039

Morishita, Y., Lazecky, M., Wright, T. J., Weiss, J. R., Elliott, J. R., & Hooper, A. (2020). LiCSBAS: An Open-Source InSAR Time Series Analysis Package Integrated with the LiCSAR Automated Sentinel-1 InSAR Processor. *Remote Sensing, 12*(3), 424. https://doi.org/10.3390/rs12030424

Marliyani, G. I. (2016). *Neotectonics of Java, Indonesia: Crustal deformation in the overriding plate of an orthogonal subduction system*. Arizona state university.

Nguyen, N., Griffin, J., Cipta, A., & Cummins, P. R. (2015). *Indonesia's Historical Earthquakes: Modelled Examples for Improving the National Hazard Map*. Geoscience Australia.

Pusat Studi Gempa Nasional. (2017). *Peta Sumber dan Bahaya Gempa Indonesia Tahun 2017*. Pusat Penelitian dan Pengembangan Perumahan dan Permukiman, Badan Penelitian dan Pengembangan, Kementerian Pekerjaan Umum dan Perumahan Rakyat.

Ramdhani, J. (2025, August 21). *BMKG: Gempa M 4,7 Bekasi Dipicu Segmen Citarum, Bukan Baribis*. DetikNews. https://news.detik.com/berita/d-8071931/bmkg-gempa-m-4-7-bekasi-dipicu-segmen-citarum-bukan-baribis

Sadly, M., Agustan, A., Yulianto, S., Bintoro, O. B., Sutrisno, D., & Alhasanah, F. (2018, September). An Application of SMART Method in vendor selection of Satellite Systems Case study of Indonesia Remote Sensing Satellite Systems (InaRSSat). In 2018 IEEE International Conference on Aerospace Electronics and Remote Sensing Technology (ICARES) (pp. 1-6). IEEE.

Suhadha, A. G., Julzarika, A., Susilo, S., Meilano, I., Syetiawan, A., & Ramdani, D. (2023). Identification of Tectonic Activity of the Baribis Fault Revealed by Present Sentinel 1 InSAR Observation. *AIP Conference Proceedings, 2941*(1), 030010. https://doi.org/10.1063/5.0181387

Susilo, S., Meilano, I., Wibowo, S. T., Syetiawan, A., Gaol, Y. A. L., Ramdani, D., & Julzarika, A. (2022). Geodetic Strain of the Baribis Fault Zone in West Java, Indonesia. *IOP Conference*

Series: Earth and Environmental Science, 1109(1), 012008. https://doi.org/10.1088/1755-1315/1109/1/012008

Susilo, S., Salman, R., Hermawan, W., Widyaningrum, R., Wibowo, S. T., Lumban-Gaol, Y. A., Meilano, I., & Yun, S. H. (2023). GNSS Land Subsidence Observations Along the Northern Coastline of Java, Indonesia. *Scientific Data, 10*(1), 329. https://doi.org/10.1038/s41597-023-02274-0

Wafid, M. (2025, August 21). *Mengenal Sesar Baribis yang Disebut Picu Gempa Bekasi M 4,7*. (Dikutip dalam DetikEdu). https://www.detik.com/edu/detikpedia/d-8071585/mengenal-sesar-baribis-yang-disebut-picu-gempa-bekasi-m-4-7

Widiyantoro, S., Supendi, P., Ardianto, A., Baskara, A. W., Bacon, C. A., Damanik, R., Rawlinson, N., Gunawan, E., Sahara, D. P., Zulfakriza, Z., Husni, Y. M., & Lesmana, A. (2022). Implications for Fault Locking South of Jakarta from an Investigation of Seismic Activity Along the Baribis Fault, Northwestern Java, Indonesia. *Scientific Reports, 12*(1), 10143. https://doi.org/10.1038/s41598-022-13896-6

Wright, T. J., Parsons, B. E., & Lu, Z. (2004). Toward Mapping Surface Deformation in Three Dimensions Using InSAR. *Geophysical Research Letters, 31*(1). https://doi.org/10.1029/2003GL018827

Yu, C., Li, Z., Chen, J., & Hu, J. C. (2018). Small Magnitude Co-Seismic Deformation of the 2017 Mw 6.4 Nyingchi Earthquake Revealed by InSAR Measurements with Atmospheric Correction. *Remote Sensing, 10*(5), 684. https://doi.org/10.3390/rs10050684